

An Expurgated Union Bound of Punctured Space-Time Turbo Codes

Luiz G. Caldeira and Cecilio Pimentel and Daniel P. B. Chaves

Abstract—This paper presents a new technique to obtain an expurgated union bound on the frame error rate of punctured space-time turbo codes (STTuC) in quasi-static Rayleigh fading channels. The STTuC scheme is composed of two component space-time trellis encoders connected in parallel via an interleaver. An adjacent matrix of an augmented state diagram is defined which allows the enumeration of each punctured component encoder. The distance spectrum of the STTuC is then obtained using the concept of uniform interleaver. A method to identify the dominant error events is proposed and an expurgated union bound on the frame error rate of STTuC schemes is computed using these dominant error events. Comparisons with simulated results reveal that the expurgated union bound is tight for codes with different construction criteria for a wide range of signal to noise ratio.

Index Terms—Space-time trellis codes, turbo codes, union bound, distance spectrum, interleaving, frame error rate, diversity, multiple antennas.

I. INTRODUCTION

The parallel concatenation of two component space-time trellis codes (STTCs) [1] combines the coding gain of turbo coding schemes [2] with the diversity gain of multiple transmit and receive antennas, resulting in a transmission scheme known as space-time turbo codes (STTuCs) [3]–[8]. STTuCs have been analyzed in schemes with high order QAM modulation in order to improve the spectral efficiency and data rates [8]–[11] considering various communications scenarios, such as cooperative communication systems [12], frequency selective channels [13], [14], underwater communications [15]. The STTuC considered in this work has two component recursive STTCs connected in parallel via an odd-even information interleaver [16]. Each component encoder produces at its output a sequence M -PSK symbols that are alternately punctured so that only one encoder accesses the transmit antennas at a given signaling interval.

Tight frame error rate (FER) bounds for STTCs over quasi-static Rayleigh fading channels have been obtained in [17]–[19] using a combination of three techniques: the enumeration of the signal matrix of error events (SMEE) together with its multiplicities (the so called distance spectrum), the derivation of the expurgated union-bound on the first error event using

a method to identify the set of dominant SMEE, and the application of the limiting-before-averaging technique on the expurgated union bound. The objective of this paper is to generalize these techniques (developed for STTCs) in order to evaluate accurate expurgated FER bounds for STTuC schemes. Previous works on this subject include [11], [20], [21]. The FER bounds derived in [20] are not only based on the distance spectrum but also on the geometric mean of the non-zero eigenvalues of the SMEE. In [11], the expurgated bound is expressed in terms of the effective product distance and Hamming distance. The bounds derived in [11], [20] are loose to predict the STTuC performance for low signal to noise ratio. In [21], the expurgated bound is about 3 dB away from the curves obtained from simulations.

The contribution of this paper is threefold. First, we define for each component STTC a product state transition diagram (PSTD) that takes into account state transitions in punctured and non-punctured intervals. This technique considers the puncturing effect by expanding the number of states of each PSTD and defines a new adjacency matrix of the extended PSTD. The symbolic algorithm proposed in [19] that algebraically manipulates the entries of the adjacency matrix of each component STTC is applied to obtain the distance spectrum of these codes. Then, we propose an STTuC enumeration that combines these spectra taking into account the interleaving effect. Finally, the dominant error events are determined and the expurgated FER bound using the limiting-before-averaging technique is numerically evaluated using these error events. The expurgated FER bound obtained with the presented technique is shown to be tight for STTuCs that employ component STTC encoders designed with different construction criteria, the determinant criterion [4] and the trace criterion [5]. Simulation results show that the bound closely matches with the simulated curves for a wide range of signal to noise ratio. It is worth mentioning that a code-search algorithm for finding the STTC constituent codes of the STTuC schemes based on EXIT charts is provided in [11].

The remainder of this paper is organized in four sections. The STTuC scheme is described in Section II. The enumeration of the SMEE spectrum taking into account the puncturing and interleaving effects is presented in Section III. Tables with the spectrum of a given order for some classical codes are also provided in this section. In section IV, the set of dominant error events in quasi-static fading is tabulated. Simulation results confirm the tightness of the expurgated bound. Concluding remarks are provided in Section V.

L. Caldeira is with the Department of Electrical Engineering and Telecommunications, Federal Institute of Education Science and Technology of Paraíba, 58015-430, João Pessoa, PB, Brazil, e-mail: guedes@ifpb.edu.br.

C. Pimentel and D. Chaves are with the Department of Electronics and Systems, Federal University of Pernambuco, Recife, PE, 50711-970, Brazil, email: {cecilio, daniel.chaves}@ufpe.br.

This work was supported in part by the Brazilian National Council for Scientific and Technological Development (CNPq) and by the Foundation for Support of Science and Technology of the State of Pernambuco (FACEPE).

Digital Object Identifier 10.14209/jcis.2018.6

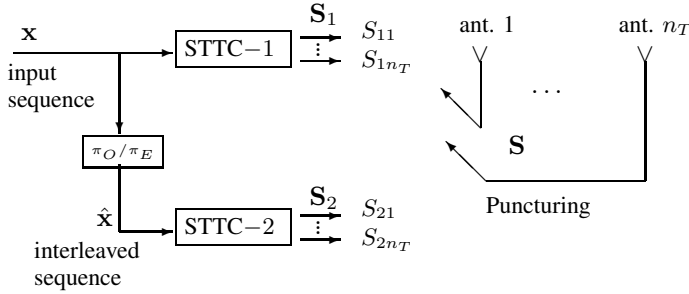


Fig. 1. STTuC scheme with two component STTCs with n_T transmit antennas. STTC outputs \mathbf{S}_1 and \mathbf{S}_2 are punctured resulting in the output sequence \mathbf{S} .

II. SPACE TIME TURBO SCHEME

Consider an STTuC scheme that employs two component STTC encoders connected in parallel via an interleaving as shown in Fig. 1. Each STTC has 2^ν states, 2^{k_c} edges emerging from each state, and transmits M -PSK symbols through n_T transmit antennas. The STTC-1 receives directly the information bits whereas the STTC-2 receives a permuted version of these bits through an interleaver of length K symbols or $K \log_2(M)$ bits. The interleaving scheme uses two half-length interleavers of odd-even type [4], [16], i.e., it interleaves, separately, symbols on odd and even positions, denoted by π_O and π_E , respectively. The length of each interleaver is $K \log_2(M)/2$ bits.

At each signaling interval, only one component STTC accesses the transmit antennas. The transmitted symbols at odd (resp. even) intervals are from STTC-1 (resp. STTC-2). Let S_{ji}^k be the output of the STTC- j transmitted by the antenna i at time k . The output of STTC-1 is the sequence $\mathbf{S}_1 = [S_{11}^k S_{12}^k \dots S_{1n_T}^k, S_{11}^{k+1} S_{12}^{k+1} \dots S_{1n_T}^{k+1}, S_{11}^{k+2} S_{12}^{k+2} \dots S_{1n_T}^{k+2}, \dots]$ and the output of STTC-2 is $\mathbf{S}_2 = [S_{21}^k S_{22}^k \dots S_{2n_T}^k, S_{21}^{k+1} S_{22}^{k+1} \dots S_{2n_T}^{k+1}, S_{21}^{k+2} S_{22}^{k+2} \dots S_{2n_T}^{k+2}, \dots]$ then the alternation of odd and even intervals during puncturing produces the transmitted sequence $\mathbf{S} = [S_{11}^k S_{12}^k \dots S_{1n_T}^k, S_{21}^{k+1} S_{22}^{k+1} \dots S_{2n_T}^{k+1}, S_{11}^{k+2} S_{12}^{k+2} \dots S_{1n_T}^{k+2}, \dots]$.

The channel is modeled as a quasi-static flat Rayleigh fading channel with an additive white Gaussian noise. The fading coefficients among the n_T transmit and n_R receive antennas are independent zero-mean complex Gaussian random variables and are constant during a transmitted frame of length K symbols and change independently from frame to frame. The fading coefficients matrix, denoted by \mathbf{H} , is given by

$$\mathbf{H} = \begin{pmatrix} h_{11} & h_{12} & \dots & h_{1n_R} \\ h_{21} & h_{22} & \dots & h_{2n_R} \\ \vdots & \dots & \ddots & \vdots \\ h_{n_T1} & h_{n_T2} & \dots & h_{n_Tn_R} \end{pmatrix}^T \quad (1)$$

where h_{ij} are the fading coefficient from transmit antenna i to receive antenna j and $(\cdot)^T$ denotes transposition.

III. PAIRWISE ERROR PROBABILITY OF AN STTC OVER QUASI-STATIC FADING CHANNELS

Assuming maximum-likelihood receiver with ideal channel state information, the conditional pairwise error probability (PEP) between a pair of correct (\mathbf{c}) and erroneous (\mathbf{e}) STTC sequences is [1]

$$P(\mathbf{c} \rightarrow \mathbf{e} | \mathbf{H}) = Q \left(\sqrt{\frac{\gamma_t}{2} \sum_{j=1}^{n_R} \mathbf{H}_j \mathbf{A}(\mathbf{c}, \mathbf{e}) \mathbf{H}_j^*} \right) \quad (2)$$

where γ_t is the signal to noise ratio (SNR) per transmit antenna, $\mathbf{H}_j = [h_{1j}, \dots, h_{n_Tj}]$ is a row vector of fading coefficients, the $n_T \times n_T$ Hermitian matrix $\mathbf{A}(\mathbf{c}, \mathbf{e})$ is the SMEE and the superscript $(\cdot)^*$ denotes conjugate transposition. For a first error event¹ of length m trellis intervals, starting at $t = 0$, the (i, j) th entry of this matrix is

$$a_{ij} = \sum_{t=0}^m (c_t^i - e_t^i) (c_t^j - e_t^j)^* \quad (3)$$

where $1 \leq i, j \leq n_T$ and c_t^i is the complex symbol transmitted from antenna i at time t chosen from an M -PSK constellation of unit energy. Hereafter, we consider $n_T = 2$, thus the 2×2 matrix $\mathbf{A}(\mathbf{c}, \mathbf{e})$ is of the form

$$\begin{pmatrix} x & z \\ z^* & y \end{pmatrix}$$

where x and y are the square Euclidean distances between the correct and erroneous symbols across each transmit antenna due to a first error event, and z is the cross-term value between the two transmit antennas defined in (3) for $i \neq j$ [17]. Define an enumerator function (also known as the transfer function) of the first error events for the component STTC- j , $j = 1, 2$, as

$$T^j(W, X, Y, Z) = \sum_{w,x,y,z} t_{w,x,y,z}^j W^w X^x Y^y Z^z \quad (4)$$

where $t_{w,x,y,z}^j$ is the average multiplicity of the first error events with Hamming distance w between the binary information sequences and x, y, z are the elements of the SMEE $\mathbf{A}(\mathbf{c}, \mathbf{e})$ corresponding to a first error event. The distance spectrum of order N of an STTuC is the ordered set $\mathcal{S} = \{(\mathbf{A}_i, a_{\mathbf{A}_i})\}_{i=1}^N$ of N dominant SMEE, where \mathbf{A}_i is an SMEE in \mathcal{S} with average multiplicity $a_{\mathbf{A}_i}$. The conditional expurgated union bound on the first error event probability becomes [19]

$$P_{fe|\mathbf{H}}(e) \simeq \sum_{\substack{i=1 \\ \mathbf{A}_i \in \mathcal{S}}}^N a_{\mathbf{A}_i} Q \left(\sqrt{\frac{\gamma_t}{2} \sum_{j=1}^{n_R} \mathbf{H}_j \mathbf{A}_i \mathbf{H}_j^*} \right). \quad (5)$$

The enumeration of the distance spectrum is performed using the PSTD of each component STTC. The states of this diagram are ordered pairs (σ_t, σ_d) called product states, where $\sigma_t, \sigma_d \in 0, 1, \dots, 2^\nu - 1$ are the states of the correct and erroneous sequences in the state diagram of the component STTC encoder, respectively. The product states are indexed

¹a path that diverge from the correct path at a fixed time instant, say $t = 0$, and remerge into this path exactly once at some time later.

from 0 to $2^{2\nu} - 1$, and they are called *good* if $\sigma_t = \sigma_d$, and *bad* otherwise. Since we are considering $n_T = 2$, each edge that connects two product states is labeled with the transition probability of the correct path, $1/2^{k_c}$, multiplied by $W^{w_i} X^{x_i} Y^{y_i} Z^{z_i}$, in which x_i , y_i , and z_i correspond to the upper diagonal portion of the SMEE due to a one-step transition in the PSTD.

The $2^{2\nu} \times 2^{2\nu}$ adjacency matrix, denoted by \mathbf{T} , associated to an STTC has the (i, j) th entry, $0 \leq i, j \leq 2^{2\nu} - 1$, either equal to the label of the edge that connects the product states S_i and S_j or zero if these states are not connected. The identification of equivalent states [23], [24] in the PSTD allows the reduction of the dimension of \mathbf{T} . Another reduction is possible by combining the *good* states into one state [25], namely S_0 . The adjacent matrix of this reduced PSTD is denoted by \mathbf{B} . Next, we split the good state into a source and a sink state, and the corresponding adjacency matrix is found by setting the $(0, 0)$ th entry of \mathbf{B} to zero, that is, $\mathbf{B}_{[0,0]} = 0$. The puncturing effect into \mathbf{B} is considered next.

Example 1: Consider an STTC with $n_T = 2$ and an adjacency matrix given by

$$\mathbf{B} = \begin{pmatrix} 0 & W^{w_0} X^{x_0} Y^{y_0} Z^{z_0} & 0 \\ W^{w_5} X^{x_5} Y^{y_5} Z^{z_5} & W^{w_1} X^{x_1} Y^{y_1} Z^{z_1} & W^{w_2} X^{x_2} Y^{y_2} Z^{z_2} \\ 0 & W^{w_3} X^{x_3} Y^{y_3} Z^{z_3} & W^{w_4} X^{x_4} Y^{y_4} Z^{z_4} \end{pmatrix}. \quad (6)$$

A. The Puncturing Effect

As the STTC- j is punctured at alternate time intervals, it is necessary to define a new PSTD, denoted by augmented state diagram [26], that indicates all possible state transitions, that is, transitions in punctured and nonpunctured intervals. The adjacency matrix of the augmented state diagram is denoted by \mathbf{B}_{punc} . In the following we describe a procedure that transforms \mathbf{B} into \mathbf{B}_{punc} .

In order to construct the augmented state diagram [26] a new set of product states $\{S'_k\}$ is added to the original PSTD, where the transitions between product states $S_i \rightarrow S'_k$ indicate puncturing occurrences (the branch labels for these transitions are equal to 1) while transitions $S'_i \rightarrow S_k$ indicate nonpuncturing occurrence (the branch labels for these transitions are the same as the original PSTD). There are no transitions $S'_i \rightarrow S'_k$ nor $S_i \rightarrow S_k$, whereas after a puncturing the encoder must transmit in the next interval and vice versa. Fig. 2 illustrates the augmented PSTD of the STTC presented in Example 1 resulting in the matrix \mathbf{B}_{punc} given by (7) shown at the top of the next page (the sequence of states in the rows/columns is $S_0, S'_1, S_1, S'_2, S_2$).

In Fig. 2 there are two edges diverging from state S_0 , one indicating puncturing and the other indicating nonpuncturing. Recall that in the first interval (an odd interval) STTC-1 transmits and STTC-2 does not transmit. The adjacency matrix $\mathbf{B}_{\text{punc}}^j$ corresponding to STTC- j is derived from \mathbf{B}_{punc} in the following way. $\mathbf{B}_{\text{punc}}^1$ is similar to its counterpart \mathbf{B}_{punc} except that the entry corresponding to the transition $S_0 \rightarrow S'_1$ on the first row of \mathbf{B}_{punc} is set to zero. Similarly, $\mathbf{B}_{\text{punc}}^2$ is obtained by setting to zero the label corresponding to $S_0 \rightarrow S_1$. Let w_O and w_E be the Hamming distance between

information sequences in odd and even intervals, respectively. These distances are enumerated separately in each STTC- j using two distinct indeterminates W_O in $\mathbf{B}_{\text{punc}}^1$ and W_E in $\mathbf{B}_{\text{punc}}^2$. For example, the matrices $\mathbf{B}_{\text{punc}}^j$ derived from (7) are given by (8) and (9) shown at the top of the next page. The matrices $\mathbf{B}_{\text{punc}}^j$ corresponding to STTC- j are the input to the algorithm presented in [19] that evaluates the transfer functions $T^1(W_O, X, Y, Z)$ and $T^2(W_E, X, Y, Z)$.

B. Interleaving Effect

We assume uniform interleavers [22] for both odd and even interleavers, i.e., all permutations in each interleaver are equally probable. The uniform interleaver π_I maps the input sequence of length $K \log_2(M)/2$ bits into all distinct permutation with equal probability $1/\binom{K \log_2(M)}{w_I}$, $I \in \{O, E\}$. The distance spectrum of order N of an STTuC is the set $\{a_{\mathbf{A}_i}^{\text{STTuC}}, a_{\mathbf{A}_i}^{\text{STTuC}}\}_{i=1}^N$. For a fixed Hamming distance $w = w_E + w_O$, the average multiplicity of an SMEE $\mathbf{A}_i^{\text{STTuC}}$ with entries $x = x_1 + x_2$, $y = y_1 + y_2$, $z = z_1 + z_2$ is given by (10) at the top of the next page, where t_{w_O, x_1, y_1, z_1}^1 is obtained from $T^1(W_O, X, Y, Z)$ and t_{w_E, x_2, y_2, z_2}^2 from $T^2(W_E, X, Y, Z)$. Thus, the average multiplicity of this SMEE $\mathbf{A}_i^{\text{STTuC}}$ (with entries x, y, z) is

$$a_{\mathbf{A}_i}^{\text{STTuC}} = \sum_w t_{w, x, y, z}^{\text{STTuC}}. \quad (11)$$

The expurgated union bound for the STTuC scheme is given by (5) using $\{a_{\mathbf{A}_i}^{\text{STTuC}}, a_{\mathbf{A}_i}^{\text{STTuC}}\}_{i=1}^N$. Table I provides the distance spectrum for the STTCs presented in [4] with modulations QPSK and 8-PSK, both with 8 states and Table II lists the set \mathcal{S} for the STTuCs presented in [5] with QPSK modulation with 4 states, and 8-PSK with 8 states. To make the tables concise, the entries of \mathbf{A}_i are listed as a vector $[a_{1,1}, a_{2,2}, a_{1,2}]$, and the two matrices $[a_{1,1}, a_{2,2}, a_{1,2}]$, $[a_{1,1}, a_{2,2}, -a_{1,2}]$ are written as $[a_{1,1}, a_{2,2}, \pm a_{1,2}]$. The notation $\mathbf{A}_{33} - \mathbf{A}_{36}$ is used to represent the matrices $\mathbf{A}_{33}, \mathbf{A}_{34}, \mathbf{A}_{35}, \mathbf{A}_{36}$. The matrices in these tables correspond to single error events with Hamming distance w up to 6 and length smaller than 10. From now on, in order to simplify the notation, we drop the superscript STTuC from \mathbf{A}_i .

The expurgated FER bound is derived using the limiting-before-averaging technique in terms of the distance spectrum

$$\text{FER} \simeq \mathbf{E} [f(\min(1, P_{\text{fe}|\mathbf{H}}(e)))] \quad (12)$$

where $f(x) = 1 - (1 - x)^K$, K is the frame length, and $\mathbf{E}[\alpha]$ is the expected value of the random variable α .

IV. DETERMINATION OF THE SET OF DOMINANT SMEE

Due to the random nature of the received SNR, the set of dominant SMEE may vary from block to block. We apply the criterion proposed in [19] to find an average set of dominant SMEE. Let $P^i(\mathbf{H})$ denote the contribution of each matrix \mathbf{A}_i to $P_{\text{fe}|\mathbf{H}}(e)$. Thus, we obtain from (5):

$$P^i(\mathbf{H}) = a_{\mathbf{A}_i} Q \left(\sqrt{\frac{\gamma t}{2} \sum_{j=1}^{n_R} \mathbf{H}_j \mathbf{A}_i \mathbf{H}_j^*} \right). \quad (13)$$

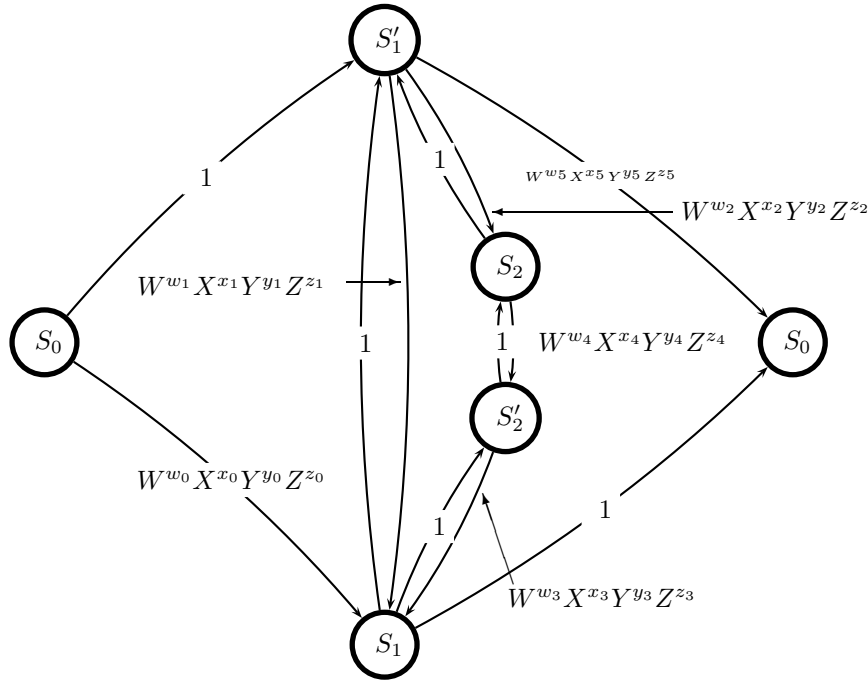


Fig. 2. Augmented state diagram of the three-state PSTD presented in Example 1, indicating puncturing and no puncturing transitions.

$$\mathbf{B}_{\text{punc}} = \begin{pmatrix} 0 & 1 & W^{w_0} X^{x_0} Y^{y_0} Z^{z_0} & 0 & 0 \\ W^{w_5} X^{x_5} Y^{y_5} Z^{z_5} & 0 & W^{w_1} X^{x_1} Y^{y_1} Z^{z_1} & 0 & W^{w_2} X^{x_2} Y^{y_2} Z^{z_2} \\ 1 & 1 & 0 & 1 & 0 \\ 0 & 0 & W^{w_3} X^{x_3} Y^{y_3} Z^{z_3} & 0 & W^{w_4} X^{x_4} Y^{y_4} Z^{z_4} \\ 0 & 1 & 0 & 1 & 0 \end{pmatrix}. \quad (7)$$

$$\mathbf{B}_{\text{punc}}^1 = \begin{pmatrix} 0 & 0 & W^{w_0} X^{x_0} Y^{y_0} Z^{z_0} & 0 & 0 \\ W^{w_5} X^{x_5} Y^{y_5} Z^{z_5} & 0 & W^{w_1} X^{x_1} Y^{y_1} Z^{z_1} & 0 & W^{w_2} X^{x_2} Y^{y_2} Z^{z_2} \\ 1 & 1 & 0 & 1 & 0 \\ 0 & 0 & W^{w_3} X^{x_3} Y^{y_3} Z^{z_3} & 0 & W^{w_4} X^{x_4} Y^{y_4} Z^{z_4} \\ 0 & 1 & 0 & 1 & 0 \end{pmatrix} \quad (8)$$

and

$$\mathbf{B}_{\text{punc}}^2 = \begin{pmatrix} 0 & 1 & 0 & 0 & 0 \\ W^{w_5} X^{x_5} Y^{y_5} Z^{z_5} & 0 & W^{w_1} X^{x_1} Y^{y_1} Z^{z_1} & 0 & W^{w_2} X^{x_2} Y^{y_2} Z^{z_2} \\ 1 & 1 & 0 & 1 & 0 \\ 0 & 0 & W^{w_3} X^{x_3} Y^{y_3} Z^{z_3} & 0 & W^{w_4} X^{x_4} Y^{y_4} Z^{z_4} \\ 0 & 1 & 0 & 1 & 0 \end{pmatrix}. \quad (9)$$

$$t_{w,x,y,z}^{\text{STuC}} = \sum_{x=x_1+x_2} \sum_{y=y_1+y_2} \sum_{z=z_1+z_2} \sum_{w=w_0+w_E} \frac{t_{w_0,x_1,y_1,z_1}^{w_0} \times t_{w_E,x_2,y_2,z_2}^{w_E}}{\left(\frac{K}{2} \log_2(M)\right)^{w_0} \left(\frac{K}{2} \log_2(M)\right)^{w_E}}. \quad (10)$$

Let $\mathcal{A}(\mathbf{H}) = \{\mathbf{A}_1, \mathbf{A}_2, \dots, \mathbf{A}_k, \dots\}$ be an ordered set of SMEE such that $P^k(\mathbf{H}) \geq P^{k+1}(\mathbf{H})$. We define the random variable X_i (which is a function of \mathbf{H}) as the position of the matrix \mathbf{A}_i in $\mathcal{A}(\mathbf{H})$. As proposed in [19], we employ the expected value of X_i , denoted by $\bar{X}_i = \mathbf{E}[X_i]$, to order the matrices in decreasing dominance. This expected value is computed from the simulations of the random matrices \mathbf{H} . For a given realization of \mathbf{H} , we calculate the ordered set $\mathcal{A}(\mathbf{H})$ using $P^i(\mathbf{H})$ in (13) for each SMEE \mathbf{A}_i shown in Tables I and II. Repeating this process for several matrices

\mathbf{H} , we calculate the average position \bar{X}_i of \mathbf{A}_i in this ordered set.

Tables III and IV present the values of \bar{X}_i for each SMEE \mathbf{A}_i considered in Tables I and II, respectively. The distinct values of \bar{X}_i form the ordered set $\beta^\iota = \{\beta_k\}_{k=1}^\iota$ with ι elements, where $\beta_k < \beta_{k+1}$. For example, we obtain from Table III (QPSK), $\beta^6 = \{17.4; 17.6; 18; 18.3; 24; 24.5\}$. Let \mathcal{S}^ι be the set of all SMEE \mathbf{A}_i such that $\bar{X}_i \in \beta^\iota$. For this set β^6 , we get from Table III that $\mathcal{S}^6 = \{\mathbf{A}_3, \mathbf{A}_{14} - \mathbf{A}_{18}, \mathbf{A}_{20}, \mathbf{A}_{31}, \mathbf{A}_{32}\}$. We denote by FER^ι the expurgated FER bound obtained with

TABLE I
SMEE OF STTuCs [4], QPSK AND 8-PSK, BOTH WITH 8 STATES.

| i (QPSK) | $\mathbf{A}_i^{\text{STTuC}}$ | $a_{\mathbf{A}_i}^{\text{STTuC}}$ | i (8-PSK) | $\mathbf{A}_i^{\text{STTuC}}$ | $a_{\mathbf{A}_i}^{\text{STTuC}}$ |
|------------|-------------------------------|-----------------------------------|-------------|--------------------------------------|-----------------------------------|
| 1, 2 | [4; 8; ± 2] | 378 | 1, 2 | [1.16; 11.4; $\pm j0.04$] | 343 |
| 3 | [6; 4; 0] | 1592 | 3, 4 | [7.96; 10.8; $\pm j3.36$] | 687 |
| 4, 5 | [8; 4; $\pm j2$] | 2280 | 5, 6 | [2.58; 9.4; ± 1.8] | 244 |
| 6, 7 | [8; 4; ± 2] | 2280 | 7, 8 | [2.58; 9.98; ± 1.38] | 176 |
| 8, 9 | [4; 8; ± 2] | 37, 84 | 9 – 12 | [1.16; 10.8; $\pm 1.48 \pm j1.42$] | 744 |
| 10, 11 | [6; 8; ± 2] | 710 | 13 – 16 | [3.98; 8.56; $\pm 1.02 \pm j2.38$] | 60 |
| 12, 13 | [4; 6; $\pm j2$] | 38, 64 | 17 – 20 | [3.98; 12; $\pm 0.96 \pm j0.4$] | 122 |
| 14, 15 | [4; 6; ± 2] | 38, 64 | 21 – 24 | [10.8; 57.96; $\pm 2.38 \pm j4.38$] | 122 |
| 16 | [4; 4; 0] | 18, 37 | 25 – 28 | [4.58; 11.3; $\pm 2.82 \pm j1.4$] | 30 |
| 17 | [6; 6; 0] | 1648 | 29 – 32 | [1.16; 11.4; $\pm 1.42 \pm j1.42$] | 122 |
| 18 | [8; 4; 0] | 7232 | 33 – 36 | [11.4; 11.3; $\pm 2.82 \pm j2$] | 160 |
| 19 | [4; 8; 0] | 652 | 37 – 40 | [3.98; 8.56; $\pm 0.4 \pm j$] | 120 |
| 20 | [4; 6; 0] | 153 | 41 – 44 | [7.96; 10.8; $\pm 1.42 \pm j4.82$] | 720 |
| 21 – 24 | [6; 6; $2 \pm j2$] | 24, 5 | | | |
| 25 – 28 | [8; 4; $2 \pm j2$] | 33, 3 | | | |
| 29, 30 | [6; 6; $\pm j2$] | 710 | | | |
| 31, 32 | [6; 4; $\pm j2$] | 33 | | | |
| 33 – 36 | [4; 8; $2 \pm j2$] | 10, 3 | | | |

TABLE II
SMEE OF STTuCs [5], QPSK (4 STATES) AND 8-PSK (8 STATES).

| i (QPSK) | $\mathbf{A}_i^{\text{STTuC}}$ | $a_{\mathbf{A}_i}^{\text{STTuC}}$ | i (8-PSK) | $\mathbf{A}_i^{\text{STTuC}}$ | $a_{\mathbf{A}_i}^{\text{STTuC}}$ |
|------------|-------------------------------|-----------------------------------|-------------|-------------------------------------|-----------------------------------|
| 1 | [22; 14; 6] | 47 | 1 – 4 | [2.58; 4; $\pm 1.58 \pm j$] | 122 |
| 2 | [22; 4; $4 + j6$] | 400 | 5 – 8 | [2.58; 4; $\pm 1 \pm j1.58$] | 122 |
| 3 | [22; 14; 8] | 178 | 9 – 12 | [2.58; 4; $\pm 1.82 \pm j0.41$] | 244 |
| 4 – 7 | [22; 4; $\pm 2 \pm j6$] | 35 | 13 – 16 | [5.41; 4; $\pm 3.82 \pm j0.41$] | 244 |
| 8 – 11 | [22; 4; $\pm j8$] | 43 | 17 – 20 | [5.41; 4; $\pm 2.41 \pm j3$] | 60 |
| 12, 13 | [22; 12; ± 4] | 41 | 21 – 24 | [5.41; 4; $\pm 3 \pm j2.41$] | 60 |
| 14 | [14; 6; $j6$] | 220 | 25 – 28 | [5.41; 4; $\pm 2.41 \pm j1.82$] | 122 |
| 15, 16 | [22; 12; $\pm j4$] | 41 | 29 – 32 | [4; 5.41; $\pm 3 \pm j0.41$] | 122 |
| 17 | [26; 8; 0] | 460 | 33 – 36 | [6; 4.58; $\pm 1.82 \pm j3.82$] | 30 |
| 18 – 21 | [20; 4; $\pm 10 \pm j2$] | 21 | 37 – 40 | [6; 4; $\pm 2.41 \pm j2.41$] | 122 |
| 22 – 25 | [10; 10; $\pm 8 \pm j4$] | 100 | 41 – 44 | [6; 4.58; $\pm 1.41 \pm j2$] | 60 |
| 26 – 29 | [20; 6; $\pm 2 \pm j12$] | 59 | 45 – 48 | [8.82; 4.58; $\pm 4.41 \pm j2.41$] | 30 |
| 30 – 33 | [22; 8; $\pm 2 \pm j8$] | 75 | 49, 50 | [3.17; 4.58; $2 \pm j2.42$] | 122 |
| 34 – 37 | [22; 8; $\pm 6 \pm j4$] | 155 | | | |
| 38 – 41 | [16; 14; $\pm 8 \pm j10$] | 325 | | | |
| 42, 43 | [22; 12; $\pm j14$] | 55 | | | |
| 44 – 47 | [20; 8; $\pm 4 \pm j2$] | 125 | | | |
| 48, 49 | [22; 8; $\pm 12 - j8$] | 330 | | | |
| 50 | [22; 6; $4 + j10$] | 35 | | | |

all SMEE in \mathcal{S}^l .

Figs. 3 and 4 show FER^l versus ι for the STTuCs [4], QPSK and 8-PSK, respectively, for two values of SNR (the FER obtained by simulations is shown in dashed lines). Similar curves are presented in Figs. 5 and 6 for the STTuC proposed in [5]. In all cases, we have found that the FER⁶ provides a good approximation to the simulated FER. So, we consider \mathcal{S}^6 as the set of dominant SMEE for all STTuC considered in this work, as is summarized in Table V. Figs. 7-10 show the expurgated FER bound versus SNR per received antenna for the STTuCs [4], [5]. As can be seen from these figures, the expurgated FER bounds have good agreement with the simulation results. The number of receive antennas (n_R) and the frame length (K) used in all simulations are $n_R = 1$, $K = 66$ for STTuCs developed in [4] and $n_R = 2$, $K = 130$ for STTuCs given in [5]. Once the set β^6 is found (for a fixed SNR), the expurgated FER bound is tight for a wide range of SNR. This is relevant in the high-SNR region, for which simulations are hard to be done. The analysis conducted in this section can be applied for other STTuCs proposed in the

literature.

V. CONCLUSIONS

A matrix-based technique to evaluate the distance spectrum of punctured STTuCs was presented in this work. We defined an adjacency matrix of an augmented state diagram which allows the enumeration of each component STTC encoder. This matrix is the input of a symbolic algorithm that evaluates the distance spectrum. The set of dominant SMEEs was classified in terms of their average individual importance to the expurgated FER bound in a quasi-static Rayleigh fading channel. We established that the dominant set \mathcal{S}^6 is robust to a wide range of SNR, number of receive antennas and code construction. Two STTuCs with design based on the determinant criterion [4] and on the trace criterion [5] were used and simulation results showed that the expurgated FER bounds are tight. An interesting direction for future work include the determination of the dominant set for STTuCs with QAM modulation [8], [14] for more general fading channels as well as the application of the technique proposed in this

TABLE III
 \bar{X}_i FOR THE STTuC CONSIDERED IN TABLE I, $n_R = 1$.

| i (QPSK) | \bar{X}_i | i (8-PSK) | \bar{X}_i |
|---------------|-------------|-------------|-------------|
| 16 | 17.4 | 5, 10, 22 | 9.3 |
| 3 | 17.6 | 6, 12 | 10.2 |
| 20 | 18 | 4, 21 | 10.5 |
| 31, 32 | 18.3 | 9, 41 | 11.1 |
| 18 | 24 | 42 | 12 |
| 14, 15, 17 | 24.5 | 2, 26, 43 | 13.8 |
| 12, 13 | 25 | 1, 44 | 14.4 |
| 4 - 7 | 24.8 | 15, 23, 24 | 15 |
| 10, 11, 19 | 25 | 8, 16, 30 | 15.3 |
| 29, 30 | 25.2 | 19, 20, 40 | 15.7 |
| 8, 9 | 26.4 | 11, 17, 31 | 16.3 |
| 25 - 28 | 26.7 | 29, 39 | 28 |
| 1, 2, 21 - 24 | 27 | 18, 27 | 28.9 |
| 33 - 36 | 29.8 | 34, 36 | 29.7 |
| | | 32 | 30.5 |
| | | 25, 37 | 31.3 |
| | | 3, 7, 35 | 32.1 |
| | | 13, 14 | 32.5 |
| | | 28, 33, 38 | 33.1 |

TABLE IV
 \bar{X}_i FOR THE STTuC CONSIDERED IN TABLE II, $n_R = 1$.

| i (QPSK) | \bar{X}_i | i (8-PSK) | \bar{X}_i |
|-----------------------------|-------------|------------------------|-------------|
| 50 | 14.7 | 6, 9 - 12 | 13 |
| 49 | 15.6 | 1 - 4, 7, 8 | 13.4 |
| 47, 48 | 16.2 | 5 | 14 |
| 46 | 17 | 15 - 21, 23, 24, 26 | 25 |
| 22, 23, 43, 45 | 18.5 | 13, 14, 22, 25, 27, 28 | 25.5 |
| 20, 21, 44 | 19 | 29 - 32 | 26.5 |
| 42 | 19.5 | 37 - 40 | 28.3 |
| 12 | 20.3 | 33 - 36 | 30.2 |
| 39 | 21.4 | 41 - 44 | 31.6 |
| 27, 37, 38, 41 | 22 | 45 - 48 | 37.4 |
| 18, 19, 24 - 26, 36, 40, 41 | 22.7 | 50 | 47 |
| 16, 17 | 23.5 | 49 | 47.8 |
| 33 - 35 | 24.5 | | |
| 30 - 32 | 25.8 | | |
| 28, 29 | 27.2 | | |
| 9 | 28.8 | | |
| 6 - 8 | 29.8 | | |
| 4, 5 | 31.5 | | |
| 2 | 32.3 | | |
| 14, 15 | 38.9 | | |
| 10, 11, 13 | 40.3 | | |
| 3 | 44.6 | | |
| 1 | 46.5 | | |

TABLE V
DOMINANT SETS \mathcal{S}^6 FOR STTuCs [4] AND [5].

| STTuC | 2^ν | Modulation | \mathcal{S}^6 |
|-------|---------|------------|---|
| [4] | 8 | QPSK | $\{\mathbf{A}_3, \mathbf{A}_{14} - \mathbf{A}_{18}, \mathbf{A}_{20}, \mathbf{A}_{31}, \mathbf{A}_{32}\}$ |
| | 8 | 8-PSK | $\{\mathbf{A}_2, \mathbf{A}_4 - \mathbf{A}_6, \mathbf{A}_9, \mathbf{A}_{10}, \mathbf{A}_{12}, \mathbf{A}_{21}, \mathbf{A}_{22}, \mathbf{A}_{26}, \mathbf{A}_{41} - \mathbf{A}_{43}\}$ |
| [5] | 4 | QPSK | $\{\mathbf{A}_{20} - \mathbf{A}_{23}, \mathbf{A}_{43} - \mathbf{A}_{50}\}$ |
| | 8 | 8-PSK | $\{\mathbf{A}_1 - \mathbf{A}_{32}\}$ |

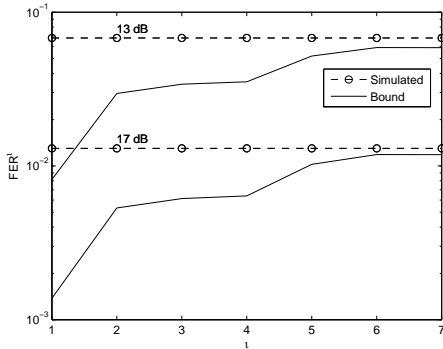


Fig. 3. $FER^l \times l$, STTuC [4], QPSK, 8 states, $n_T = 2$, $n_R = 1$, $K = 66$, SNR = 13 dB and 17 dB.

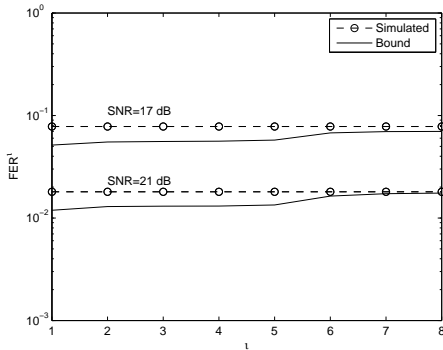


Fig. 4. $FER^l \times l$, STTuC [4], 8-PSK, 8 states, $n_T = 2$, $n_R = 1$, $K = 66$, SNR = 17 dB and 21 dB.

work to develop bounds on the bit error probability (BER). The derivation of FER/BER bounds for LDPC-based space-time codes [27] can also be studied in the future.

REFERENCES

- [1] V. Tarokh, N. Seshadri, and A. R. Calderbank, "Space-time codes for high data rate wireless communication: Performance criteria and code construction," *IEEE Trans. Inf. Theory*, vol. 44, no. 2, pp. 744-765, Mar. 1998, doi: 10.1109/18.661517.
- [2] C. Berrou and A. Glavieux, "Near optimum error correcting coding and decoding: Turbo-codes," *IEEE Trans. Commun.*, vol. 44, no. 10, pp. 1261-1271, Oct. 1996, doi:10.1109/26.539767.
- [3] H. J. Su and E. Geraniotis, "Space-time turbo codes with full antenna diversity," *IEEE Trans. Commun.*, vol. 49, no. 1, pp. 47-57, Jan. 2001, doi: 10.1109/26.898250.
- [4] D. Tujkovic, M. Juntti, and M. Latva-aho, "Space-time turbo coded modulation: design and applications," *EURASIP J. Appl. Signal Proc.*, vol. 2002, no. 1, pp. 236-248, Jan. 2002, doi: 10.1155/S1110865702000641.
- [5] Y. Hong, J. Yuan, Z. Chen, and B. Vucetic, "Space-time turbo trellis codes for two, three, and four transmit antennas," *IEEE Trans. Veh. Technol.*, vol. 53, no. 2, pp. 318-328, Mar. 2004, doi: 10.1109/TVT.2004.823549.
- [6] H. Chen, A. M. Haimovich, and J. Sjögren, "Turbo space-time codes with time varying linear transformations," *IEEE Trans. Wireless Commun.* vol. 6, no. 2, pp. 486-493, Feb. 2007, doi: 10.1109/TWC.2007.04790.

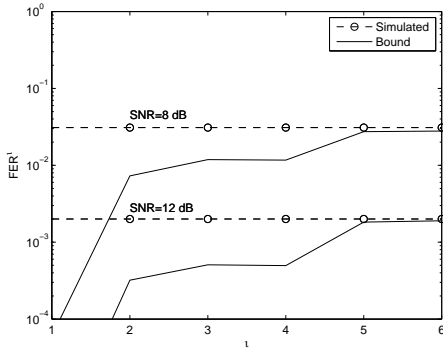


Fig. 5. $FER^l \times l$, STTuC [5], QPSK, 4 states, $n_T = 2$, $n_R = 2$, $K = 130$, SNR = 8 dB and 12 dB.

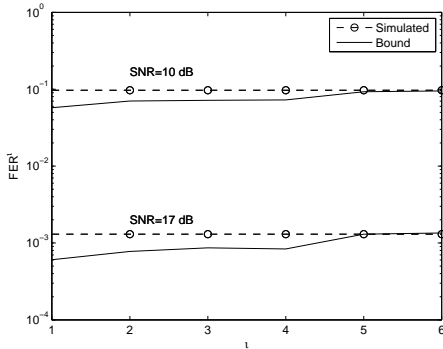


Fig. 6. $FER^l \times l$, STTC [5], 8-PSK, 8 states, $n_T = 2$, $n_R = 2$, $K = 130$, SNR = 10 dB and 17 dB.

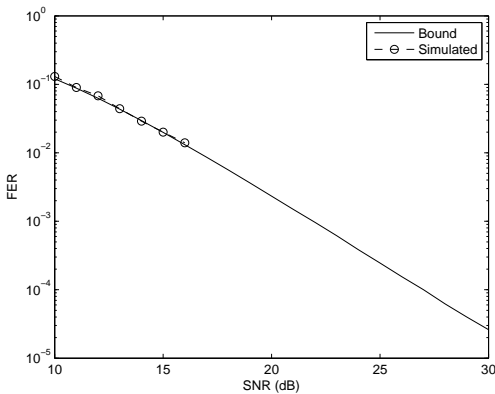


Fig. 7. $FER \times SNR$ for STTuC [4], QPSK, 8 states, $n_T = 2$, $n_R = 1$, $K = 66$, and Rayleigh fading channel. The set of dominant SMEE is $S^6 = \{\mathbf{A}_3, \mathbf{A}_{14} - \mathbf{A}_{18}, \mathbf{A}_{20}, \mathbf{A}_{31}, \mathbf{A}_{32}\}$.

[7] M. Sellathurai and S. Haykin, *Space-Time Turbo Codes and Turbo Decoding Principles*, John Wiley & Sons, Inc., 2009.

[8] A. Rotopanescu, L. Trifina, and D. Tarniceriu, "Soft estimates for doubly iterative decoding of space-time turbo codes using M-ary quadrature amplitude modulation," in *Proc. International Symposium on Signals, Circuits and Systems (ISSCS)*, pp.1-4, 2017, doi: 10.1109/ISSCS.2017.8034868.

[9] A. Bassou, A. Djebbari, and M. Benaissa, "Design of unpunctured turbo trellis-coded modulation," *AEU - International Journal of Electronics and Communications*, vol. 67, no.3, pp. 223-232, Mar. 2013, doi: 10.1016/j.aeue.2012.08.005.

[10] F. Khalili, "Design and simulation of coded-modulation using turbo trellis coding and multi-layer modulations," Ph.D. thesis, School of

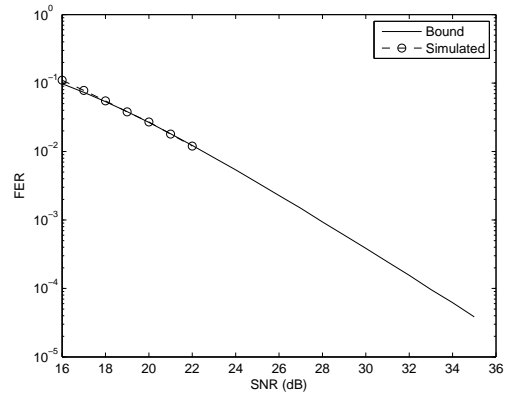


Fig. 8. $FER \times SNR$ for STTuC [4], 8-PSK, 8 states, $n_T = 2$, $n_R = 1$, $K = 66$, and Rayleigh fading channel. The set of dominant SMEE is $S^6 = \{\mathbf{A}_2, \mathbf{A}_4 - \mathbf{A}_6, \mathbf{A}_9, \mathbf{A}_{10}, \mathbf{A}_{12}, \mathbf{A}_{21}, \mathbf{A}_{22}, \mathbf{A}_{26}, \mathbf{A}_{41} - \mathbf{A}_{43}\}$.

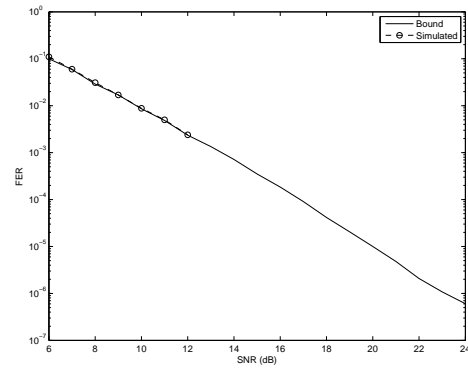


Fig. 9. $FER \times SNR$ for STTuC [5], QPSK, 4 states, $n_T = 2$, $n_R = 2$, $K = 130$, and Rayleigh fading channel. The set of dominant SMEE is $S^6 = \{\mathbf{A}_{20} - \mathbf{A}_{23}, \mathbf{A}_{43} - \mathbf{A}_{50}\}$.

Electrical Engineering and Computer Science, Ohio University, USA, 2017.

[11] S. X. Ng, O. R. Alamri, Y. Li, J. Kliewer, and L. Hanzo, "Near-capacity turbo trellis coded modulation design based on EXIT charts and union bounds," *IEEE Trans. Commun.*, vol. 56, no. 12, pp. 2030-2039, Dec. 2008, doi: 10.1109/TCOMM.2008.06039522.

[12] H. Sun, S. X. Ng, and L. Hanzo, "Turbo trellis-coded hierarchical-modulation assisted decode-and-forward cooperation," *IEEE Trans. Veh. Technol.*, vol. 64, no. 9, pp. 3971-3981, Sept. 2015, doi: 10.1109/TVT.2014.2366689.

[13] K. S. Vishvaksean and D. Abidha, "Performance of turbo coded space-time transmit diversity aided IDMA system," *International Conference on Communications and Signal Processing (ICCS)*, pp.1-5, 2015, doi: 10.1109/ICCS.2015.7322533.

[14] A. Bassou, A. Hasni, and A. M. Lakhdar, "UTTCM-based optimization of coded communication system," *American Journal of Computation, Communication and Control*, vol. 1, no. 3, Sept. 2014.

[15] N. Iruthayanathan, K.S. Vishvaksean, V. Rajendran, and S. Mohankumar, "Performance analysis of turbo-coded MIMO - OFDM system for underwater communication," *Computers & Electrical Engineering*, vol. 43, pp. 1-8, April 2015, doi: 10.1016/j.compeleceng.2015.01.018.

[16] K. S. Arkoudogiannis, C.E. Dimakis, and K. V. Koutsouvelis, "A better understanding of the performance of rate-1/2 binary turbo codes that use odd-even interleavers," *International Symposium on Communication Systems, Networks and Digital Signal Processing*, Poznan, Poland, pp. 1-6, 2012.

[17] A. Stefanov and T. M. Duman, "Performance bounds for space-time trellis codes," *IEEE Trans. Inf. Theory*, vol. 49, no. 9, pp. 2134-2140, Sept. 2003, doi: 10.1109/TIT.2003.815773.

[18] A. P. des Rosiers and P. H. Siegel, "On performance bounds for space-time codes on fading channels," *IEEE Trans. Commun.*, vol. 52, no.

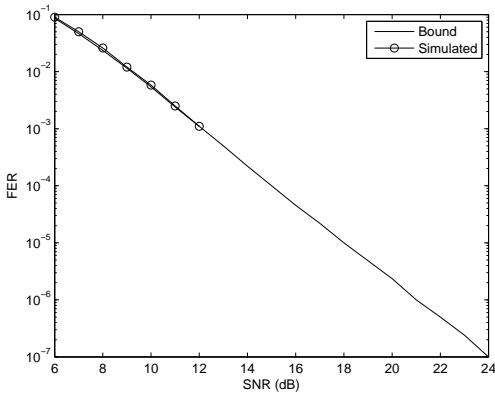


Fig. 10. FER \times SNR for STTuC [5], 8-PSK, 8 states, $n_T = 2$, $n_R = 2$, $K = 130$, and Rayleigh fading channel. The set of dominant SMEE is $S^6 = \{\mathbf{A}_1 - \mathbf{A}_{32}\}$.



Cecilio Pimentel was born in Recife, Brazil, in 1966. He received the B.Sc. degree from the Federal University of Pernambuco, Recife, Brazil, in 1987; the M.Sc. degree from the Catholics University of Rio de Janeiro, Rio de Janeiro, Brazil, in 1990; and the Ph.D. degree from the University of Waterloo, Ontario, Canada, in 1996, all in electrical engineering. Since October 1996, he has been with the Department of Electronics and Systems at the Federal University of Pernambuco, where he is currently a Full Professor. From 2007 to 2008, he was a Visiting Research Scholar at the Department of Mathematics and Statistics, Queen's University, Kingston, Canada. His research interests include digital communications, information theory, chaos-based communication, and error correcting coding. He is a Senior Member of the Brazilian Telecommunications Society (SBTr) and is a Senior Member of the IEEE.

10, pp. 1688-1697, Oct. 2004, doi: 10.1109/TCOMM.2004.836429.

[19] L. G. Caldeira and C. Pimentel, "Distance spectrum and expurgated union bound of space-time trellis codes in quasi-static Rician Fading Channels," *IEEE Trans. Veh. Technol.*, vol. 58, no. 9, pp. 5264-5269, Nov. 2009, doi: 10.1109/TVT.2009.2023790.

[20] D. Tujkovic, "Space-time turbo coded modulation: analysis and code optimization over fading channels," *Asilomar Conference on Signals, Systems and Computers*, California, USA, pp. 146-150, 2003, doi: 10.1109/ACSSC.2003.1291887.

[21] A. Stefanov and T. M. Duman, "Performance bounds for turbo-coded multiple antenna systems," *IEEE J. Select. Areas Commun.*, vol. 21, no. 3, pp. 374-371, Apr. 2003, doi: 10.1109/JSAC.2003.809695.

[22] S. Benedetto and G. Montorsi, "Unveiling turbo-codes: Some results on parallel concatenated coding schemes," *IEEE Trans. Inf. Theory*, vol. 42, no. 2, pp. 409-428, Mar. 1996, doi: 10.1109/18.485713.

[23] C. Schlegel, *Trellis Coding*. New York:IEEE Press, 1997.

[24] W. E. Ryan and Z. Tang, "Reduced-complexity error state diagrams in TCM and ISI channel performance evaluation," *IEEE Trans. Commun.*, vol. 52, no. 12, pp. 2047-2051, Dec. 2004, doi: 10.1109/TCOMM.2004.838674.

[25] J. Shi and R. D. Wesel, "Efficient computation of trellis code generating functions," *IEEE Trans. Commun.*, vol. 52, no. 2, pp. 219-227, Feb. 2004, doi: 10.1109/TCOMM.2003.822702.

[26] I. Chatzigeorgiou, M. R. D. Rodrigues, I. J. Wassel, and R. A. Carrasco "The augmented state diagram and its application to convolutional and turbo codes," *IEEE Trans. Commun.*, vol. 57, no. 7, pp. 1948-1958, Jul. 2009, doi: 10.1109/TCOMM.2009.07.070344.

[27] K. Wang, H. Shen, and W. Wu, and Z. Ding, "Joint detection and decoding in LDPC-based space-time coded MIMO-OFDM systems via linear programming," *IEEE Trans. Signal Process.*, vol. 63, no. 13, pp. 3411 - 3424, July 2015, doi: 10.1109/TSP.2015.2422681.



Daniel P. B. Chaves received the the B.S. degree in electronics engineering and the M.S. degree in electrical engineering from the Federal University of Pernambuco, Recife, Brazil, in 2004 and 2006, respectively, and the Ph.D. degree in electrical engineering from the State University of Campinas, São Paulo, Brazil, in 2011. In 2012, he joined the Department of Electronics and Systems, Federal University of Pernambuco, Recife, Brazil, as a Assistant Professor. His current interests include information theory, coding theory, symbolic dynamics, system modeling, chaos communication, chaotic circuits and chaos based random number generators.



Luiz G. Caldeira received the B.Sc. degree from the Federal University of Mato Grosso, Cuiabá, Brazil, in 1993; the M.Sc. and the Doctor degrees from the Federal University of Pernambuco, Recife, Brazil, in 2002 and 2011, respectively, all in electrical engineering. Since February 1987, he has been with the Department of Electrical Engineering at the Federal Institute of Paraíba. His research interests include digital communications, compressed sensing, coding theory.